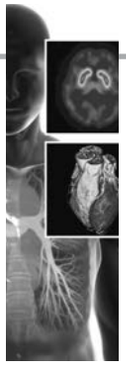

What challenges must be overcome before ultrasound elasticity imaging is ready for the clinic?

Ultrasound elasticity imaging has been a research interest for the past 20 years with the goal of generating novel images of soft tissues based on their material properties (i.e., stiffness and viscosity). The motivation for such an imaging modality lies in the fact that many soft tissues can share similar ultrasonic echogenicities, but may have very different mechanical properties that can be used to clearly visualize normal anatomy and delineate diseased tissues and masses. Recently, elasticity imaging techniques have moved from the laboratory to the clinical setting, where clinicians are beginning to characterize tissue stiffness as a diagnostic metric and commercial implementations of ultrasonic elasticity imaging are beginning to appear on the market. This article provides a foundation for elasticity imaging, an overview of current research and commercial realizations of elasticity imaging technology and a perspective on the current successes, limitations and potential for improvement of these imaging technologies.

KEYWORDS: acoustic radiation force ■ elasticity ■ shear wave ■ stiffness ■ strain ■ ultrasound

Mark L Palmeri[†1,2] & Kathryn R Nightingale[1]

[1]Department of Biomedical Engineering, Duke University, Durham, NC 27708, USA
[2]Department of Anesthesiology, Duke University, Durham, NC 27708, USA
[†]Author for correspondence:
Tel.: +1 919 660 5158
Fax: +1 919 684 4488
mark.palmeri@duke.edu

Soft tissue material properties

Manual palpation of tissue has been a diagnostic tool used by doctors for centuries. The value of manual palpation in this setting lies in the fact that pathologic processes, such as the growth of malignant tumors or scarring of tissues, involves replacing healthy tissues with fibrotic tissue or increasing the cellular density of tissues that are, in general, stiffer than the surrounding tissues. The stiffness of tissues can be described by their Young's modulus (E), which is a measure of a material's resistance to compressive deformation [1]. Tissues with higher Young's moduli, such as muscle and fibrous tissue, are more resistant to deformation than more compliant tissues, such as fat [2–4]. Tissue deformations occur in response to a stress (σ) being applied to the tissues; in the case of manual palpation, this stress is related to the force exerted by the clinician's fingers over the surface area of an organ or mass. The deformation that occurs in response to this applied stress is known as the strain (ε).

While soft tissues are very complex, heterogeneous materials, many assumptions are made in the field of elasticity imaging to simplify the analysis and interpretation of elasticity images [5,6]. Common material assumptions include that the tissue is: linear (i.e., the amount of strain resulting from an applied incremental stress is not a function of the absolute stress applied), elastic (i.e., the tissue returns back to its nondeformed state when an applied stress is removed and the deformation state is not dependent on the rate of the applied stress), isotropic (i.e., the tissue's material properties are not orientation dependent) and incompressible (i.e., the volume of the tissue remains the same when strained due to its high water content). Under these assumptions, stress and strain can be related to each other by the Young's modulus [1]:

$$\sigma = E\,\varepsilon \qquad (1)$$

Some elasticity imaging modalities do not make as many assumptions about tissue material properties; two common deviations from these assumptions include modeling the tissue as being viscoelastic and being nonlinear. The introduction of viscosity to the tissue description allows the tissue stiffness to be a function of the excitation frequency (i.e., $E(f)$), where higher frequency excitations yield a stiffer tissue response compared with lower frequency excitations. These viscous mechanisms also result in energy loss in the tissue. Tissue nonlinearities imply that the strain in response to an applied stress is dependent on the absolute stress that is applied to the tissue (i.e., Young's modulus is a function of strain, $E(\varepsilon)$).

Elasticity imaging modalities generate images of tissue stiffness [5,6]. They accomplish this by applying a stress to the tissues, either using an external excitation source, an internal, physiologic motion source or acoustic radiation force and measuring the resulting deformation (displacement) in response to that stress. Based on a stress/strain relationship, such as that in Equation 1, this measured deformation in response to the applied stress can be related to the tissue stiffness.

future medicine part of fsg

■ Stress sources

Elasticity imaging requires a source of stress to deform tissue so that relative or absolute responses to that stress can be measured to generate elasticity images. These excitation sources can be external to the body and include mechanical punches, vibrating rods and compression plates. In ultrasound elasticity imaging, the ultrasound transducer can be used to apply compression to the tissues of interest through the skin surface. The benefit of this excitation source is that known stresses (or strains) can be applied to large volumes of tissue, which can be useful when screening tissues for lesions. A potential drawback to external excitation can be limited coupling of these applied stresses into deep organs of interest (e.g., the liver in an obese patient) due to attenuation of the stress from the skin surface or a physical barrier to coupling that stress into deep organs, such as the presence of abdominal ascites.

To overcome the challenge of coupling stress into internal organs of interest, some imaging modalities utilize internal sources of motion, such as cardiac, arterial or respiratory motion, to generate stress in organs of interest. While these stress sources are internal and coupled nicely to adjacent organs, these stresses are complex, difficult to quantify and variable through time. Regardless of these challenges, many imaging modalities, especially those characterizing cardiac [7–10] and vascular tissues [11,12], successfully utilize these sources of stress to generate elasticity images.

A unique stress source available to ultrasound elasticity imaging is acoustic radiation force. Acoustic radiation force results from a transfer of momentum from the propagating ultrasonic wave to the sound absorbing soft tissue. This momentum transfer results in a body force in the direction of the wave propagation and through the use of longer and/or stronger acoustic pulses than are typically used in diagnostic ultrasound, transient tissue deformation on the order of microns can be generated. The acoustic radiation force (F) is a body force (i.e., a force applied over a volume of material) that can be related to the acoustic attenuation of the tissue (α), the acoustic intensity (I) and the sound speed (c) by [13,14]:

$$F = \frac{2\alpha I}{c} \quad (2)$$

The spatial distribution of this acoustic radiation force is the same as the acoustic intensity field generated by a focused ultrasound transducer [15].

For all of the nonphysiologic stress sources outlined above, theses stresses can be applied (quasi) statically, where a stress state is applied and held or dynamically, where the stress is applied impulsively (i.e., a transient excitation typically lasting tens-to-hundreds of microseconds) or harmonically (i.e., a sinusoid of one or more frequencies).

■ Displacement/strain estimation

Ultrasound elasticity imaging relies on acquiring raw radio-frequency (RF) data before and after a stress has been applied to the tissue to measure the deformation in response to that stress. Traditional displacement estimation techniques include normalized cross correlation (NCC) methods [16] and phase-shift estimators [17,18].

Ultrasound imaging has very good resolution in the axial dimension (the direction of acoustic wave propagation), allowing displacements on the order of single microns to be measured; however, the displacement resolution in the orthogonal directions is typically an order-of-magnitude worse as it is related to the acoustic beamwidth at the focus (tenths to single millimeters) [19].

Some elasticity imaging modalities use the displacement data (u) to measure the dynamic response of the tissues; however, others compute the strain (ε) from these displacements:

$$\varepsilon = \frac{1}{2}(\nabla u)^T + \nabla u) \quad (3)$$

where ∇u represents the spatial displacement gradient and ^{T} represents the transpose operation. Typically these strain values are directly displayed in elastograms, where under the assumption of uniform stress, they are indicative of stiffness (Equation 1) or these strains are used as inputs for inverse material models to reconstruct the material stiffness images [20]. While these strains have traditionally been axial strains (i.e., deformations in the direction of tissue compression), more recent efforts have focused on shear strain and axial shear strain (strains orthogonal to the direction of compression) estimation as a means of characterizing additional information about the connectivity of lesions to their surrounding tissues [21–23]. This would be analogous to a clinician evaluating the mobility of a lesion with manual palpation, which can provide differential information because mobile lesions tend to be benign and anchored lesions tend to have more aggressive desmoplastic reactions that tether them to surrounding tissues [22,23].

■ Shear waves

Another approach to elasticity imaging involves generating shear waves that propagate through tissue and imaging their propagation using either ultrasound or magnetic resonance imaging [24–30]. Shear waves propagate in a direction

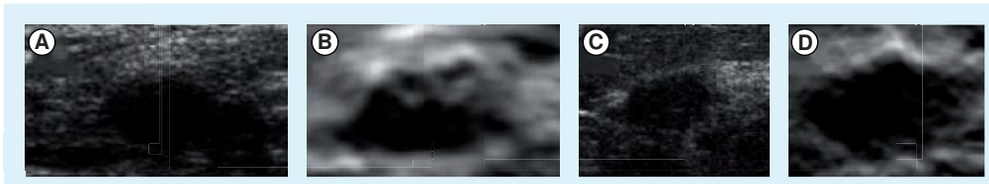

Figure 1. B-mode images and their corresponding strain elastograms in the breast.
(A & B) Fibroadenoma that is **(A)** clearly hypoechoic in the B-mode image and **(B)** delineated as a discrete region of decreased strain (i.e., darker and, therefore, stiffer), in the corresponding elastogram **(B)**. **(C & D)** Cancer that is hypoechoic with **(C)** deep shadowing in the B-mode image and **(D)** appears as a lower strain (i.e., stiffer) region in the elastogram, although the size is significantly increased, possibly representing the desmoplastic response around this malignant mass.
Courtesy of Dr Timothy Hall.

orthogonal to the direction of the induced displacement (in contrast to acoustic compressive waves that propagate in the same direction as the particle compression). Shear waves can be generated using external sources such as a vibrating plate [26] or a mechanical punch [31] or using acoustic radiation force [27]. These shear waves propagate several orders-of-magnitude slower than acoustic waves; therefore, they can be imaged with high frame rates using ultrasound imaging and can also be imaged using MRI.

The speed of propagating shear waves (c_T) can be related to the shear modulus (μ) by:

$$C_T = \sqrt{\frac{\mu}{\rho}} \quad (4)$$

where ρ represents the soft tissue mass density (typically 1.0 g/cm^3). The shear modulus (μ) in Equation 4 can be related to the Young's modulus (E) in Equation 1 by:

$$E = 3\mu \quad (5)$$

under the assumptions of the soft tissue being an incompressible, linear, elastic, isotropic solid. Using the displacement estimation techniques previously mentioned, the shear waves resulting from impulsive acoustic radiation force excitations can be tracked through time and space by using ultrasound tracking beams that are spatially offset from the excitation [27–30]. There are also implementations of shear wave imaging that rely on the interference patterns of multiple shear wave sources, as is done in sonoelastography [32].

Current research & commercial implementations

■ Compressive elastography

Ophir *et al.* originally proposed generating qualitative images of tissue strain in response to compressive stress as a means of imaging the stiffness of soft tissues [33]. Many researchers have been investigating the use of compressive elastography to identify masses and to characterize their status as benign or malignant based on their material properties. Hall *et al.* has been studying the use of elastography in the breast to help distinguish benign fibroadenomas from malignant masses (Figure 1) [34]. There have also been efforts to specifically use tissue nonlinearity as a mechanism to differentiate benign from malignant masses [35].

There are also studies using compressive elastography in the setting of characterizing deep vein thromboses, where compressive ultrasonic evaluation is already the clinical gold standard, to differentiate young clots from older clots based on their stiffness [36]. The same technology is also being studied to differentiate inflammation from scarring in the setting of inflammatory bowel disease [37].

Hitachi Medical Systems introduced one of the first commercial implementations of compressive elastography with their real-time tissue elastography (RTE) tool that was introduced in 2003. The clinical utility of this imaging mode

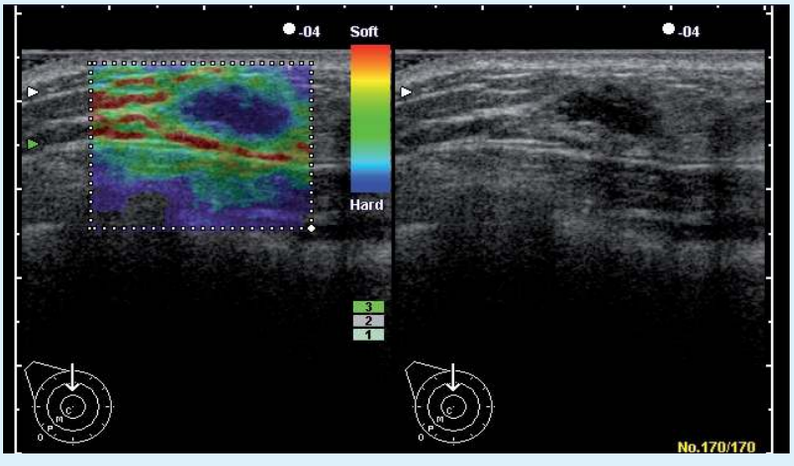

Figure 2. Biopsy-confirmed invasive ductal carcinoma in the breast Hitachi Real-time Tissue Elastography tool. The mass is identified as a region of reduced strain (blue) in the elastogram, indicating that it is stiff and differentiating from benign masses such as fibroadenomas that typically have more uniform elastograms with adjacent healthy breast tissue.
Courtesy of Hitachi Medical Systems.

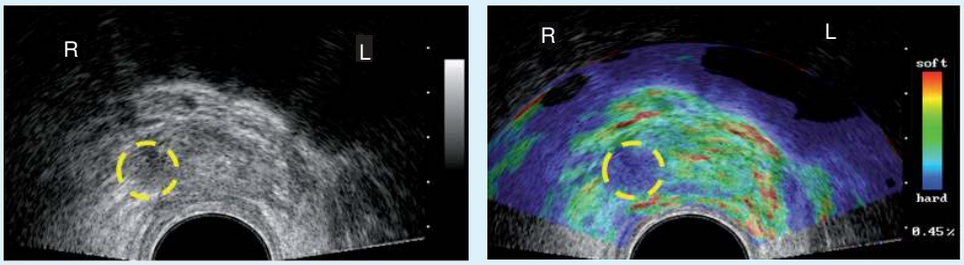

Figure 3. B-mode and elastogram images of a prostate in a 79-year-old male with a PSA of 19.0 who had a negative digital rectal exam. The B-mode image has a slightly hypoechoic region on the right lobe of the prostate (left side of the image) that appears as a uniform blue (region of decreased strain, therefore stiffer) in the elastogram (delineated with the dashed yellow circles). Pathology indicated that this mass was a carcinoma in the transition zone of the prostate.
Courtesy of Hitachi Medical Systems and Professor Akaza, Tsukuba University Hospital, Japan.

has been evaluated in the breast (Figure 2) and prostate (Figure 3), demonstrating the potential clinical utility for strain elastograms to differentiate benign from malignant masses [38–40].

Compressive elastography imaging modes are now also available on the Siemens Medical Solutions ACUSON Antares™ and S2000™ ultrasound scanners as eSie Touch™ elasticity imaging [41], the GE Healthcare Logiq E9 elastography mode [101] and the Philips iU22 elastography mode [102].

■ Acoustic radiation force imaging

Acoustic radiation force impulse (ARFI) imaging relies on acoustic radiation force to transiently deform soft tissues and the resulting

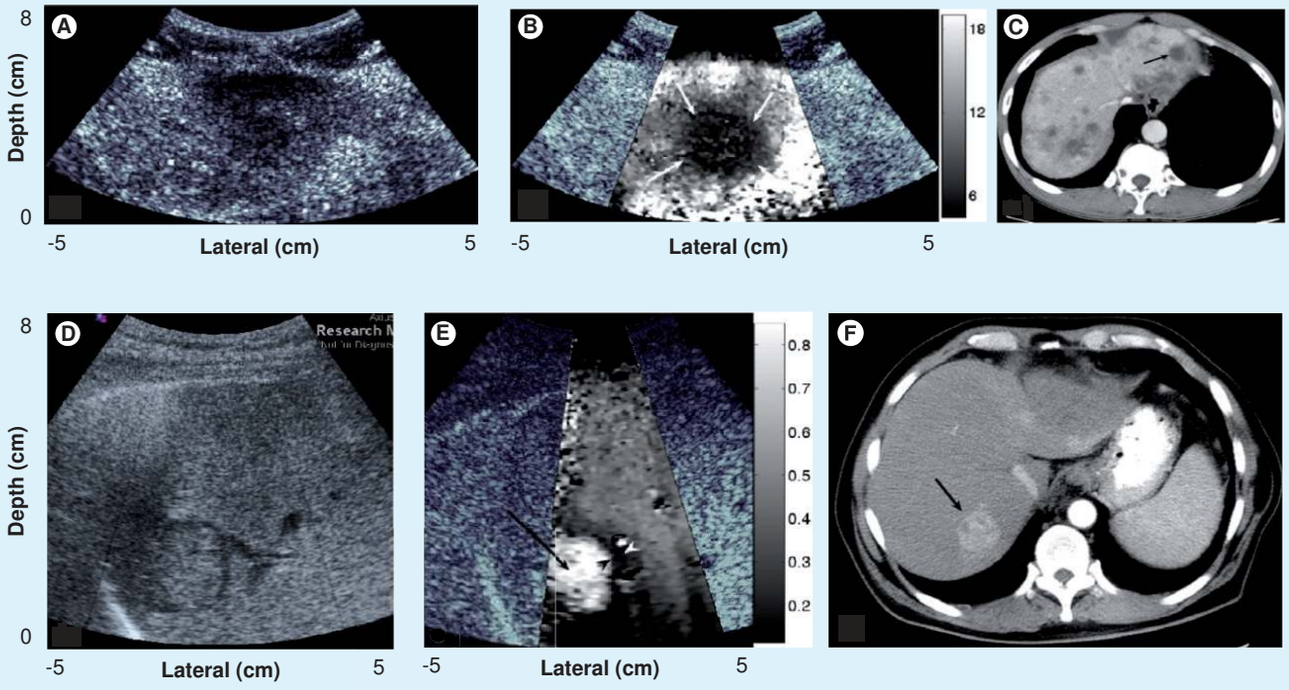

Figure 4. B-mode, acoustic radiation force impulse and CT images of liver masses in healthy and fibrotic livers. Top row of images shows a metastatic melanoma mass in an otherwise healthy liver background. **(A)** The mass appears as a hypoechoic region in the B-mode image; **(B)** in the corresponding acoustic radiation force impulse (ARFI) image, the malignant mass does not displace as much as the background liver tissue and can be interpreted to be stiffer than the liver tissue. **(C)** This mass is also identified as a region of reduced opacity on the corresponding CT image, indicated with an arrow. **(D)** The images in the bottom row show B-mode and **(E)** ARFI displacement images of a hepatocellular carcinoma in a fibrotic liver. In the ARFI image, the mass appears more compliant (i.e., displaces more) than the stiffer, diseased liver tissue. **(F)** The corresponding CT image for this hepatocellular carcinoma, with the lesion indicated with an arrow. The colorbars in the ARFI images represent displacement in microns.
Reproduced with permission from [42] © (2008) *Physics in Medicine and Biology*.

displacement fields can be used to generate images of relative stiffness over the region of interest. Figure 4 shows images of liver masses in a study by Fahey *et al.*, where the masses have different displacement contrast relative to the background liver tissue depending on the health of that liver tissue [42].

Other clinical applications of ARFI imaging that have been studied include the prostate, where zonal anatomy and cancerous regions can be identified [43], along with breast mass imaging [44], gastrointestinal tract imaging [45], regional anesthesia guidance [46], monitoring the growth of thermal ablation lesions [47] and characterizing cardiac [48] and vascular tissues [49–51].

As demonstrated in Figures 1–4, qualitative elasticity images display relative tissue stiffness; quantifying absolute tissue stiffness of different disease states is not possible with these relative imaging modalities, which has motivated the development of quantitative shear wave imaging. These qualitative images do, however, provide improved contrast that can be used concurrently with the B-mode images to improve the visualization of anatomic structures and lesions.

Siemens Medical Solutions has implemented a version of ARFI imaging on their ACUSON S2000™ ultrasound scanner as the Virtual Touch™ Tissue Imaging tool. Clinical studies in Europe and Asia are actively being conducted to evaluate the clinical utility of this imaging modality [52]. There are also implementations of acoustic radiation force-based elasticity imaging that characterize material properties through harmonic excitations, as opposed to impulsive excitations. Vibroacoustography (VA) [53] and harmonic motion imaging (HMI) [54] are two such modalities that vibrate tissue using acoustic radiation force and then generate images based on the amplitude and frequency response of the tissue to those excitations.

The use of acoustic radiation force methods to characterize materials is also being researched for *in vitro* applications, where novel devices, such as the sonorheometer, are being used to characterize blood coagulation in the operating room setting for timely feedback to anesthesiologists and surgeons [55].

■ Qualitative elasticity image artifacts

Similar to shadowing, reverb and clutter artifacts that can be present in B-mode images, elasticity images are susceptible to their own artifacts that clinicians must be trained to accommodate during their interpretation. Tissue compression can lead to strain concentration artifacts around structures that can lead to distortions in the strain fields [56]; a common example of this is demonstrated in a shear strain image of a stiff, spherical inclusion in Figure 5 [21].

More complex structures will have equally complex strain artifacts surrounding them that challenge direct strain-to-stiffness image interpretation.

In the qualitative acoustic radiation force-based imaging modalities, dependencies on focal gain and acoustic attenuation create gradients in the acoustic radiation force field that directly modulate the resultant displacement magnitudes [57]. In these settings, focal gain displacement normalization can be applied to simplify the interpretation of displacement as being inversely proportional to stiffness, still under the assumption of uniform acoustic attenuation in these regions of interest. A demonstration of how this displacement normalization can be performed is shown in Figure 6.

When transient excitations are used to generate qualitative displacement images (e.g., ARFI images), attention must be paid to what time after the excitation is being evaluated due to the contrast reversal and changes in apparent structural size that can occur later in the transient response [58]. Current commercial applications of ARFI imaging typically restrict image display to the early times after excitation where displacement amplitude can be more closely interpreted as being inversely proportional to stiffness.

■ Shear wave (quantitative) imaging

The inability for relative or qualitative stiffness images to provide absolute stiffness information provides challenges when trying to diagnose disease state based on stiffness metrics and when trying to longitudinally follow changes in

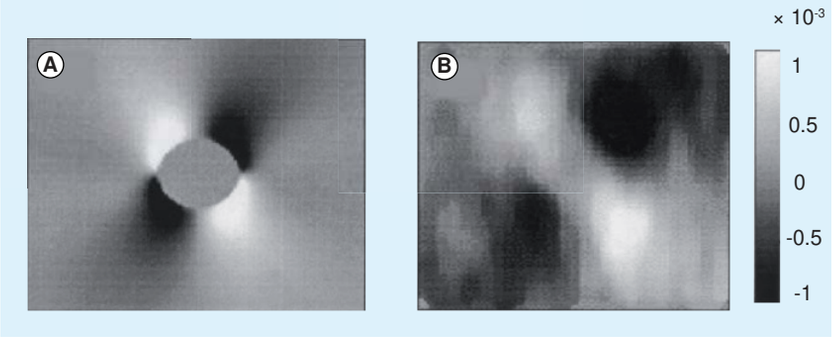

Figure 5. Compressive elastography strain concentration artifacts. (A) Shear strain image of a spherical inclusion twice as stiff as the background material simulated using finite elements; **(B)** estimated shear elastogram using the simulated data. The colorbar represents the amount of strain.
Reproduced with permission from [21] © (2000) *Ultrasonics*.

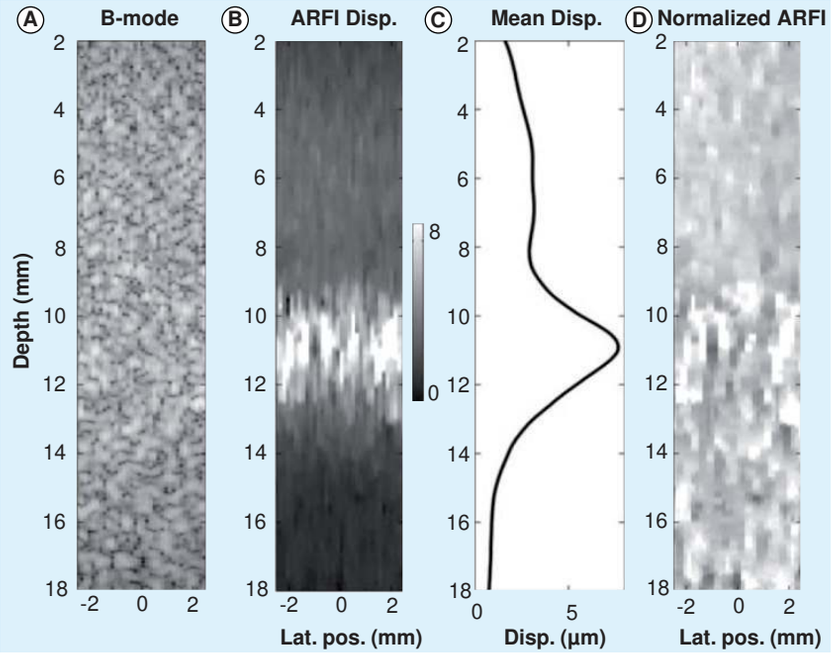

Figure 6. Acoustic radiation force impulse image displacement normalization demonstrated in a homogeneous tissue-mimicking phantom. **(A)** The B-mode image shows a region of phantom with homogeneous stiffness and acoustic attenuation (0.7 dB/cm/MHz); **(B)** the corresponding acoustic radiation force impulse image 0.3 ms after a radiation force excitation focused at 11 mm with an F/1.3 focal configuration shows the impact of focal gain on the resulting displacement profile. **(C)** After normalizing by the mean displacement amplitude as a function of depth, **(D)** a more uniform normalized displacement image is achieved. ARFI: Acoustic radiation force impulse.
Reproduced with permission from [57] © (2006) *Ultrasound in Medicine and Biology.*

stiffness since other confounding factors may affect the relative images (e.g., acoustic attenuation). Sarvazyan *et al.* proposed a method for quantifying the absolute shear modulus of soft tissue using the shear waves that are generated from an impulsive acoustic radiation force excitation [27] and experimental implementations with the associated shear wave estimation algorithms were subsequently developed [28,30]. ARFI imaging has been extended to provide quantitative stiffness metrics by measuring the arrival time of shear waves at spatially offset positions from the radiation force excitation [28,59,60] and has been used to evaluate the possibility of diagnosing liver fibrosis using noninvasive liver stiffness measurements instead of liver biopsy in patients being evaluated for nonalcoholic fatty liver disease (NAFLD), with promising data showing the ability to differentiate advanced fibrosis/cirrhosis from mild to no liver fibrosis (Figure 7) [61]. These trends are similar to those provided by other elasticity imaging modalities, such as FibroScan ([62] discussed below) and magnetic resonance elastography (MRE), which are starting to be used in place of biopsy to noninvasively characterize liver stiffness [63].

EchoSens has developed a dedicated stiffness characterization system, the FibroScan®, to quantify liver stiffness. This system relies on a mechanical punch to generate shear waves that propagate from the skin surface down into the liver and the speed of these propagating shear waves is measured with ultrasonic tracking techniques, as discussed. While this system does not provide ultrasonic imaging capabilities, it has received appreciable usage in Europe and Asia, particularly in studying liver fibrosis in patients with hepatitis C and fatty liver disease [62,64]. Siemens Medical Solutions has also implemented a version of ARFI shear wave imaging on their ACUSON S2000® ultrasound scanner as the Virtual Touch™ Tissue Quantification tool. This is actively being studied and compared with the FibroScan® system to measure liver stiffness in a variety of liver diseases with very encouraging results [65].

Recently, SuperSonic Imagine released the Aixplorer® ultrasound scanner that generates quantitative elasticity images based on shear wave propagation measurements for shear waves generated with impulsive acoustic radiation force. This ultrasound scanner is based on the SuperSonic Imaging (SSI) technology developed by Fink *et al.* [30]. Initial clinical applications of the Aixplorer® have been in characterizing breast lesions (Figure 8) [66] and the system is actively being translated to applications in the liver, thyroid and prostate.

There are active research efforts looking at more complex radiation force-derived shear wave excitation sources to improve the accuracy and resolution of these techniques, such as spatially modulus ultrasound radiation force (SMURF) by McAleavey *et al.* [67] and higher-order reconstruction [68–70]. Additionally, several groups are investigating the use of more complex material models to derive additional information about tissue viscoelasticity [29,71].

■ Quantitative elasticity imaging artifacts

While static, qualitative strain-based elasticity imaging has been actively researched for almost 20 years, newer quantitative imaging methods based on shear wave propagation are still being established. Many of these modalities have been developed under the assumption of tissue homogeneity (at least over specific regions of interest); however, additional studies should presented in the literature that assess the validity of these modalities when they are applied to image structures such as masses or layered organs. In these settings, the boundary

conditions and interference patterns associated with shear wave reflections and transmission can compromise the accuracy of these shear wave reconstruction approaches, which could lead to artifacts that could complicate image/metric interpretation [72]. Application of these technologies beyond the targets for which they were developed should involve control studies to establish the validity of the measurements in new settings.

Future perspective

Elasticity imaging has extensive clinical potential in the fields of diagnostics and monitoring. There has been demonstrated success in the fields of tissue ablation monitoring where ultrasound elasticity imaging can improve the lesion contrast and border delineation over B-mode imaging, providing the clinician with additional information during these interventional procedures [47,73–78]. Two common locations for tissue ablation include the liver and the heart. In the liver, CT imaging can usually visualize the lesions of interest, but CT imaging cannot easily be used during an ablation procedure and it is typically delayed postprocedure to allow for localized tissue swelling to abate. The fact that ablated tissue stiffens provides a unique niche for ultrasound elasticity imaging techniques to be used for real-time feedback during the procedures, especially in the setting where B-mode contrast of these growing lesions does not become appreciable until bubbles have formed and adjacent healthy tissue has been charred [73]. Fluoroscopy and intravascular B-mode guidance is typically used when RF ablations are used to treat arrhythmogenic foci in the heart. Unfortunately, B-mode imaging does not clearly delineate ablation lesions as they form, but similar to the stiffening of liver tissue that occurs during ablations, cardiac tissue also stiffens when ablated, providing a unique opportunity for ultrasound elasticity imaging to help interventional cardiologists during these procedures to localize their lesions while sparing adjacent healthy myocardial tissue [47].

With every new clinical technology, clinical studies need to be performed to establish the technology's clinical utility, educate clinicians on interpreting these new data and caution clinicians about the limitations of those interpretations. As exemplified in the liver mass study by Fahey *et al.* (Figure 4) [42], relative elasticity images have several layers of interpretation beyond the initial observation and conclusion that more strain/displacement means the target structure is more compliant. It can be difficult to determine if the stiffness of a lesion or the background tissue has changed when evaluating these relative stiffness images. Even so, the clear delineation of lesion boundaries and the increased contrast over B-mode images provides significant additional clinical information.

To make quantitative elasticity imaging a viable and useful clinical tool, large-scale studies need to be performed to establish elasticity (stiffness) metrics for healthy and diseased tissues. The current literature contains stiffness values for soft tissues that span a wide range that limits the utility of these metrics to glean clinical information [2,4,79–81]. Given that many assumptions are being made in the current commercial implementations of elasticity imaging (e.g., soft tissues are linear and purely elastic), these stiffness metrics need to be accompanied with information about the modes of excitation (e.g., static vs dynamic, small vs large strain or frequency of excitation, for example) that could be used to help compare/contrast these different imaging methods and establish a foundation for higher-order material models to be used for tissue stiffness reconstructions.

Stiffness metrics also need to be established as a function of disease state and patient demographic. While there are many hypotheses for why tissues stiffen or soften in the face of disease (e.g., scarring of the liver leads to increased fibrotic tissue that is stiffer), these

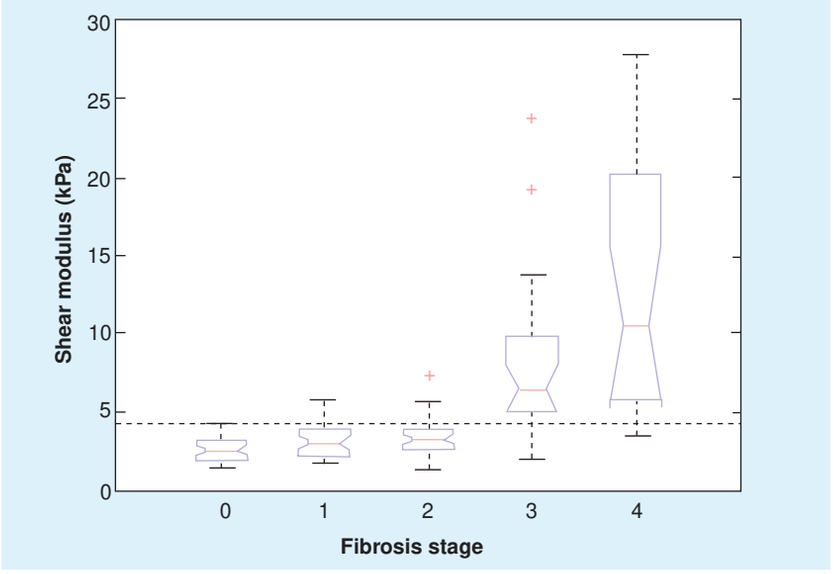

Figure 7. Liver stiffness, as characterized using acoustic radiation force impulse shear wave imaging, as a function of biopsy-proven fibrosis stage in patients being evaluated for nonalcoholic fatty liver disease. Choosing a shear stiffness threshold of 4.24 kPa allowed F3–4 fibrosis stages (advanced fibrosis and cirrhosis) to be distinguished from mild to no fibrosis (F0–2) with 90% sensitivity and specificity (AUC = 0.90).
Data from [61].

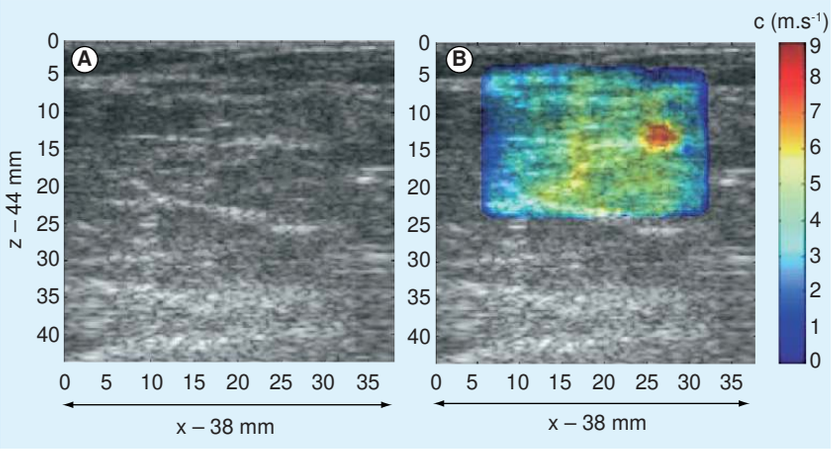

Figure 8. Characterization of a 5 mm grade III infiltrating ductal carcinoma using SuperSonic Imaging. (A) The B-mode image shows a slightly hypoechoic region that is clearly delineated as stiff (red) in **(B)** the corresponding shear velocimetry map.
Reproduced with permission from [66] © (2008) *Ultrasound in Medicine and Biology.*

disease processes may exhibit differences in their mechanical manifestation based on the etiology of the disease, pre-existing conditions and other variables associated with the patient's overall health such as blood pressure or perfusion, for example. That being said, ultrasound elasticity imaging has demonstrated great clinical promise in the fields of noninvasively diagnosing liver fibrosis with the FibroScan®, Virtual Touch® Tissue Quantification and Aixplorer® systems in the settings of viral hepatitis and fatty liver disease and additional clinical niches are being explored in the fields of breast lesion characterization using the Airxplorer® system [66].

The clinical potential for quantitative ultrasonic elasticity imaging can be seen in the current applications of MRE [63,82–84]. A very comprehensive review of MRE has been prepared by Mariappan *et al.* [63], which demonstrates the clinical utility of MRE in the area of diagnosing liver fibrosis without needing liver biopsy. Additionally, MRE is being investigated to image pathologies in the brain, breast, blood vessels, heart, kidneys and skeletal muscle and some organs that ultrasound is not amenable to imaging, such as lung. Ultimately, it may prove that MRE and ultrasound elasticity imaging methods may be synergistic in the clinical environment and satisfy different niches (e.g., real-time imaging and guidance with ultrasound versus improved soft tissue contrast and 3D tissue screening with MRE).

The study of more complex material models to represent soft tissues will also open new doors of clinical opportunity as additional metrics to differentiate disease states are defined. In addition to tissue nonlinearity, soft tissues are known to be viscoelastic and frequency-based tissue responses have been demonstrated in liver and breast tissue by techniques such as Shearwave Dispersion Ultrasound Vibrometry (SDUV) [29] and Shear Wave Spectroscopy [71,85], in addition to the MRE literature [63]. Additionally, given that water is known to redistribute throughout soft tissue, more complex poroelastic tissue models are also being explored to evaluate inflammation and lymphedema that may further expand the clinical applications for ultrasound elasticity imaging [86–89].

There are additional technical innovations that can be made to improve the likelihood that ultrasound elasticity will have clinical success and utility. As obesity becomes more prevalent in Western societies, the ability to image at depth becomes more of a concern. Many target organs for elasticity imaging, such as the liver and kidney, become increasingly difficult to image as the amount of subcutaneous and visceral fat between the ultrasound transducer and the target organs increases. Adipose tissue can be highly attenuating, reducing the ultrasound SNR at depth, which degrades conventional B-mode image quality, compromising the ability to accurately estimate displacement and strain and reducing acoustic radiation force amplitudes. Improvements in transducer technology to achieve greater acoustic output without lens heating will allow stronger and longer ultrasound pulses to be delivered to the tissue without risking transducer damage [90]. Additionally, improvements in displacement and strain estimation in the presence of noisy signals will allow for improved elasticity imaging without necessarily increasing the acoustic exposure to patients. More advanced algorithms are actively being studied by many research groups [91–93].

It is likely that the 'difficult to image patient' could be successfully imaged with stronger and longer ultrasonic pulses for deeper B-mode imaging and for acoustic radiation force-based imaging modalities; however, most systems are using the maximum US FDA-allowed acoustic output. Therefore, the current diagnostic ultrasound safety limits imposed by the FDA would need to be revisited in the context of applying these elasticity imaging methods in the obese, 'difficult to image' population. Current diagnostic ultrasound limits are based on the acoustic output limits that were possible decades ago;

more comprehensive studies involving the bioeffects of short-duration, radiation force-based pulses need to be performed in the context of thermal exposure and cavitation risk, as are currently regulated via the thermal index (TI) [94], mechanical index (MI) and spatial-peak-temporal-average intensity. These limits are actively being studied [94–97] and revising these guidelines could open more doors of opportunity for radiation force-based ultrasonic elasticity imaging in challenging patient populations. While in the research setting there has been no anecdotal evidence of adverse events in limited clinical tests that have been performed with moderately elevated acoustic output limits [61], revisiting clinical limits may require additional bioeffect analyses.

Overall, the future of ultrasound elasticity imaging in the clinical setting is very bright. Successful studies demonstrating the utility of elasticity imaging have been performed in the context of characterizing cancerous lesions in the breast, prostate, liver and thyroid, staging liver fibrosis noninvasively, evaluating venous clots, visualizing tissue inflammation/scarring and in monitoring thermal ablation procedures. Even more clinical opportunities will be generated as additional and future-generation commercial implementations of these technologies are made available to clinicians to facilitate large-scale studies for a variety of disease processes. The fact that ultrasound elasticity imaging also provides real-time feedback in a cost-effective manner, without the use of ionizing radiation, will also become appealing in the future as healthcare costs need to be reduced and new concerns to reduce patient and physician exposure to radiation are addressed in medical centers around the world.

Acknowledgements

The authors would like to thank Pamela Anderson and Taylor Jordan for their assistance in formatting images and text for this article. Special thanks to the journals IEEE Transactions on Ultrasonics, Ferroelectrics and Frequency Control, Ultrasound in Medicine and Biology, *and* Ultrasonics and Physics in Medicine and Biology *for figure reproduction permission and Timothy Hall for use of his data.*

Financial & competing interests disclosure

The authors are inventors of the ARFI imaging technology and Duke University holds associated intellectual property rights. The ARFI imaging research has been supported by NIH grants R01 EB002312 and R01 CA142824. ARFI imaging technology has been implemented commercially by Siemens Medical Solutions on their ACUSON S2000™ ultrasound scanner as Virtual Touch™ Tissue Imaging and Quantification tools. The authors have no other relevant affiliations or financial involvement with any organization or entity with a financial interest in or financial conflict with the subject matter or materials discussed in the manuscript apart from those disclosed.

No writing assistance was utilized in the production of this manuscript.

Executive summary

- Ultrasound elasticity images of soft tissue stiffness are generated by measuring the displacements/strains that result from an applied stress.
- Sources of stress include physiologic motion, tissue compression with the ultrasound transducer and focused acoustic radiation force excitations in the tissues of interest.
- Real-time relative tissue stiffness images can be generated and related to stiffness under several material assumptions.
- Real-time quantitative soft tissue stiffnesses and stiffness images can be reconstructed by measuring the propagation speed of shear waves resulting from transient acoustic radiation force excitations or mechanical vibrations.

Current research & commercial implementations

- Qualitative elasticity images can provide better contrast and spatial resolution than B-mode images in some cases.
- Quantitative elasticity data can be used to longitudinally monitor disease state and to potentially evaluate disease severity (e.g., liver fibrosis, benign vs malignant distinction).
- Large-scale studies need to be performed to characterize the stiffness of healthy and diseased soft tissues, especially in the presence of confounding factors such as blood pressure and operator dependencies.
- Ultrasound stiffness images can contain artifacts, similar to those present in B-mode images, that clinicians must be trained to interpret (e.g., strain concentration artifacts or acoustic radiation force attenuation dependencies).

Future perspective

- Diagnostic ultrasound transducers and associated safety limits need to be re-evaluated in the context of acoustic radiation force-based imaging modalities to extend their application to patients who are difficult to image (e.g., high BMI).
- The assumptions surrounding soft tissue stiffness reconstructions and the associated image artifacts when they are violated need to be evaluated, especially when technologies are applied to new clinical problems for which they were not developed.
- Ultrasound elasticity imaging has strong clinical potential in the future as a safe, cost-effective means of diagnosis and disease monitoring.

Bibliography

Papers of special note have been highlighted as:
- ▪ of interest
- ▪▪ of considerable interest

1 Lai R. *Introduction to Continuum Mechanics*. Butterworth-Heinmann, Woburn, MA, USA (1999).

2 Duck F. *Physical Properties of Tissue, A Comprehensive Reference Book*. Academic Press, NY, USA (1990).

3 Sarvazyan A, Skovaroda AR, Emelianov SY *et al.* Biophysical bases of elasticity imaging. *Acoust. Imaging* 21, 223–240 (1995).

4 Sarvazyan A. Elastic properties of soft tissue. In: *Handbook of Elastic Properties of Solids, Liquids and Gases.* 107–127 (2001).

5 Greenleaf JF, Fatemi M, Insana M. Selected methods for imaging elastic properties of biological tissues. *Annu. Rev. Biomed. Eng.* 5, 57–78 (2003).

▪ **Overview of imaging modalities to characterize soft tissue stiffness.**

6 Parker KJ, Taylor LS, Gracewski S, Rubens DJ. A unified view of imaging the elastic properties of tissue. *J. Acoust. Soc. Am.* 117(5), 2705–2712 (2005).

▪ **Overview of imaging modalities to characterize soft tissue stiffness.**

7 Heimdal A, Støylen A, Torp H, Skjaerpe T. Real-time strain rate imaging of the left ventricle by ultrasound. *J. Am. Soc. Echocardiogr.* 11(11), 1013–1019 (1998).

8 Konofagou EE, D'Hooge J, Ophir J. Myocardial elastography – a feasibility study *in vivo*. *Ultrasound Med. Biol.* 28(4), 475–482 (2002).

9 D'hooge J, Bijnens B, Thoen J, Van de Werf F, Sutherland GR, Suetens P. Echocardiographic strain and strain-rate imaging: a new tool to study regional myocardial function. *IEEE Trans. Med. Imaging* 21(9), 1022–1030 (2002).

10 Sutherland GR, Di Salvo G, Calus P, D'hooge J, Bijnens B. Strain and strain rate imaging: a new clinical approach to quantifying regional myocardial function. *J. Am. Soc. Echocardiogr.* 17(7), 788–802 (2004).

11 de Korte CL, van der Steen AF. Intravascular ultrasound elastography: an overview. *Ultrasonics* 40(1–8), 859–865 (2002).

12 de Korte CL, Woutman HA, van der Steen AF, Pasterkamp G, Céspedes EI. Vascular tissue characterisation with IVUS elastography. *Ultrasonics* 38(1–8), 387–390 (2000).

13 Nyborg L. Acoustic Streaming. In: *Physical Acoustics.* Mason WP (Ed.). Academic Press Inc, NY, USA, 265–331 (1965).

14 Torr GR. The acoustic radiation force. *Am. J. Phys.* 52, 402–408 (1984).

15 Nightingale K, Palmeri M. Acoustic Radiation Force Impulse (ARFI) imaging: fundamental concepts and image formation. In: *Biomedical Applications of Vibration and Acoustics in Imaging and Characterizations.* Fatemi M, Al-Jumaily A (Eds.). ASME Press, NY, USA, 77–91 (2008).

16 Pinton GF, Dahl JJ, Trahey GE. Rapid tracking of small displacements with ultrasound. *IEEE Trans. Ultrason. Ferroelec. Freq. Contr.* 53(6), 1103–1117 (2006).

17 Loupas T, Peterson R, Gill R. Experimental evaluation of velocity and power estimation for ultrasound blood flow imaging, by means of a two-dimensional autocorrelation approach. *IEEE Trans. Ultrason. Ferroelec. Freq. Contr.* 42(4), 689–699 (1995).

18 Kasai C, Namekawa K, Koyano A, Omoto R. Real-time two-dimensional blood flow imaging using an autocorrelation technique. *IEEE Trans. Ultrason. Ferroelec. Freq. Contr.* SU-32(3), 458–463 (1985).

19 Cobbold RS. *Foundations of Biomedical Ultrasound*. Oxford University Press, Oxford, UK (2007).

20 Barbone PE, Oberai AA. Elastic modulus imaging: some exact solutions of the compressible elastography inverse problem. *Phys. Med. Biol.* 52(6), 1577–1593 (2007).

21 Konofagou E, Harrigan T, Ophir J. Shear strain estimation and lesion mobility assessment in elastography. *Ultrasonics* 38, 400–404 (2000).

22 Thitaikumar A, Mobbs LM, Kraemer-Chant CM, Garra BS, Ophir J. Breast tumor classification using axial shear strain elastography: a feasibility study. *Phys. Med. Biol.* 53(17), 4809–4823 (2008).

23 Thittai A, Galaz B, Ophir J. Axial-shear strain distributions in an elliptical inclusion model: experimental validation and *in vivo* examples with implications to breast tumor classification. *Ultrasound Med. Biol.* 36(5), 814–820 (2010).

24 Kemper J, Sinkus R, Lorenzen J, Nolte-Ernsting C, Stork A, Adam G. MR elastography of the prostate: initial *in-vivo* application. *Rofo* 176(8), 1094–1099 (2004).

25 Sinkus R, Tanter M, Xydeas T, Catheline S, Bercoff J, Fink M. Viscoelastic shear properties of *in vivo* breast lesions measured by MR elastography. *Magn. Reson. Imaging* 23(2), 159–165 (2005).

26 Huwart L, Sempoux C, Salameh N *et al.* Liver fibrosis: non-invasive assessment with MR elastography. *NMR Biomed.* 19(2), 173–179 (2006).

27 Sarvazyan A, Rudenko OV, Swanson SD, Fowlkes JB, Emelianov SY. Shear wave elasticity imaging: a new ultrasonic technology of medical diagnostics. *Ultrasound Med. Biol.* 24(9), 1419–1435 (1998).

▪▪ **One of the original papers describing the use of propagating shear waves to reconstruct soft tissue elasticity.**

28 Palmeri ML, Wang MH, Dahl JJ, Frinkley KD, Nightingale KR. Quantifying hepatic shear modulus *in vivo* using acoustic radiation force. *Ultrasound Med. Biol.* 34(4), 546–558 (2008).

29 Chen S, Urban M, Pislaru C *et al.* Shearwave dispersion ultrasound vibrometry (SDUV) for measuring tissue elasticity and viscosity. *IEEE Trans. Ultrason. Ferroelectr. Freq. Control.* 56(1), 55–62 (2009).

30 Bercoff J, Tanter M, Fink M. Supersonic shear imaging: a new technique for soft tissue elasticity mapping. *IEEE Trans. Ultrason. Ferroelectr. Freq. Control.* 51(4), 396–409 (2004).

31 Sandrin L, Tanter M, Gennisson JL, Catheline S, Fink M. Shear elasticity probe for soft tissues with 1-D transient elastography. *IEEE Trans. Ultrason. Ferroelectr. Freq. Control.* 49(4), 436–446 (2002).

32 Taylor LS, Porter BC, Rubens DJ, Parker KJ. Three-dimensional sonoelastography: principles and practices. *Phys. Med. Biol.* 45, 1477–1494 (2000).

33 Ophir J, Céspedes I, Ponnekanti H, Yazdi Y, Li X. Elastography: a quantitative method for imaging the elasticity of biological tissues. *Ultrasonic Imaging* 13(2), 111–134 (1991).

▪▪ **One of the original papers describing compressive ultrasound elastography.**

34 Burnside ES, Hall TJ, Sommer AM *et al.* Differentiating benign from malignant solid breast masses with US strain imaging. *Radiology* 245(2), 401–410 (2007).

35 Hall TJ, Oberait AA, Barbone PE *et al.* Elastic nonlinearity imaging. *Proc. IEEE Eng. Med. Biol. Soc.* 1967–1970 (2009).

36 Rubin JM, Xie H, Kim K *et al.*, Sonographic elasticity imaging of acute and chronic deep venous thrombosis in humans. *J. Ultrasound Med.* 25(9), 1179–1186 (2006).

37 Kim K, Johnson LA, Jia C. Noninvasive ultrasound elasticity imaging (UEI) of Crohn's disease: animal model. *Ultrasound Med. Biol.* 34(6), 902–912 (2008).

38 Aigner F, Pallwein L, Junker D *et al.* Value of real-time elastography targeted biopsy for prostate cancer detection in men with prostate specific antigen 1.25 ng/ml or greater and 4.00 ng/ml or less. *J. Urol.* 184(3), 913–917 (2010).

39 Aigner F, Mitterberger M, Rehder P *et al.* Status of transrectal ultrasound imaging of the prostate. *J. Endourol.* 24(5), 685–691 (2010).

40 Zhi H, Ou B, Luo BM, Feng X, Wen YL, Yang HY. Comparison of ultrasound elastography, mammography, and sonography in the diagnosis of solid breast lesions. *J. Ultrasound Med.* 26(6), 807–815 (2007).

41 Lazebnik RS. Tissue strain analytics and virtual touch tissue imaging and quantification. *White Paper.* (2008).

42 Fahey B, Nelson RC, Bradway DP, Hsu SJ, Dumont DM, Trahey GE. *In vivo* visualization of abdominal malignancies with acoustic radiation force elastography. *Phys. Med. Biol.* 53, 279–293 (2008).

43 Zhai L, Madden J, Foo WC, Palmeri ML, Mouraviev V, Polascik TJ, Nightingale KR. Acoustic radiation force impulse imaging of human prostates *ex vivo*. *Ultrasound Med. Biol.* 36(4), 576–588 (2010).

44 Congdon A, Soo MS, Trahey GE, Nightingale KR. Acoustic radiation force impulse (ARFI) imaging of *in vivo* breast masses. *Proc. IEEE Eng. Med. Biol. Soc.* 1, 728–731 (2004).

45 Palmeri ML, Frinkley K, Zhai L *et al.* Acoustic Radiation Force Impulse (ARFI) imaging of the gastrointestinal tract. *Ultrasonic Imaging* 27, 75–88 (2005).

46 Palmeri ML, Dahl JJ, MacLeod DB, Grant SA, Nightingale KR. Improving regional nerve visualization with acoustic radiation force impulse (ARFI) imaging. Presented at: *ASA 2008 Annual Meeting.* Orlando, FL, USA, 20 October 2008.

47 Eyerly SA, Hsu SJ, Agashe SH, Trahey GE, Li Y, Wolf PD. An *in vitro* assessment of acoustic radiation force impulse imaging for visualizing cardiac radiofrequency ablation lesions. *J. Cardiovasc. Electrophysiol.* 21(5), 557–563 (2010).

48 Hsu SJ, Bouchard R, Dumont DM, Wolf PD, Trahey GE. *In vivo* assessment of myocardial stiffness with acoustic radiation force impulse imaging. *Ultrasound Med. Biol.* 33(11), 1706–1719 (2007).

49 Trahey GE, Palmeri ML, Bentley RC, Nightingale KR. Acoustic radiation force impulse imaging of the mechanical properties of arteries: *in vivo* and *ex vivo* results. *Ultrasound Med. Biol.* 30(9), 1163–1171 (2004).

50 Dumont D, Dahl J, Miller E, Allen J, Fahey B, Trahey G. Lower-limb vascular imaging with acoustic radiation force elastography: demonstration of *in vivo* feasibility. *IEEE Trans. Ultrason. Ferroelectr. Freq. Control.* 56(5), 931–944 (2009).

51 Dahl JJ, Dumont DM, Allen JD, Miller EM, Trahey GE. Acoustic radiation force impulse imaging for noninvasive characterization of carotid artery atherosclerotic plaques: a feasibility study. *Ultrasound Med. Biol.* 35(5), 707–716 (2009).

52 Cho S, Lee JY, Han JK, Choi BI. Acoustic radiation force impulse elastography for the evaluation of focal solid hepatic lesions: preliminary findings. *Ultrasound Med. Biol.* 36(2), 202–208 (2010).

53 Fatemi M, Greenleaf J. Vibro-acoustography: an imaging modality based on utrasound-stimulated acoustic emission. *Proc. Natl Acad. Sci. USA* 96, 6603–6608 (1999).

54 Vappou J, Maleke C, Konofagou EE. Quantitative viscoelastic parameters measured by harmonic motion imaging. *Phys. Med. Biol.* 54(11), 3579–3594 (2009).

55 Viola F, Kramer MD, Lawrence MB, Oberhauser JP, Walker WF. Sonorheometry: a noncontact method for the dynamic assessment of thrombosis. *Ann. Biomed. Eng.* 32(5), 696–705 (2004).

56 Barbone PE, Bamber JC. Quantitative elasticity imaging: what can and cannot be inferred from strain images. *Phys. Med. Biol.* 47(12), 2147–2164 (2002).

57 Nightingale K, Palmeri M, Trahey G. Analysis of contrast in images generated with transient acoustic radiation force. *Ultrasound Med. Biol.* 32(1), 61–72 (2006).

58 Palmeri ML, Sharma AC, Bouchard RR, Nightingale RW, Nightingale KR. A finite-element method model of soft tissue response to impulsive acoustic radiation force. *IEEE Trans. Ultrason. Ferroelectr. Freq. Control.* 52(10), 1699–1712 (2005).

59 Wang MH, Palmeri ML, Rotemberg VM, Rouze NC, Nightingale KR. Improving the robustness of time-of-flight based shear wave speed reconstruction methods using RANSAC in human liver *in vivo*. *Ultrasound Med. Biol.* 36(5), 802–813 (2010).

60 Rouze NC, Wang MH, Palmeri ML, Nightingale KR. Robust estimation of time-of-flight shear wave speed using a radon sum transformation. *IEEE Trans. Ultrason. Ferroelectr. Freq. Control.* 57(12), 2662–2670 (2010).

61 Palmeri ML, Wang MH, Rouze NC *et al.* Noninvasive evaluation of hepatic fibrosis using acoustic radiation force-based shear stiffness in patients with nonalcoholic fatty liver disease. *J. Hepatol.* DOI: 10.1016/j.jhep.2010.12.019 (2011) (Epub ahead of print).

62 Yoneda M, Fujita K, Inamori M, Tamano M, Hiriishi H, Nakajima A. Transient elastography in patients with non-alcoholic fatty liver disease (NAFLD). *Gut* 56(9), 1330–1331 (2007).

63 Mariappan YK, Glaser KJ, Ehman RL. Magnetic resonance elastography: a review. *Clin. Anat.* 23(5), 497–511 (2010).

▪ **Comprehensive review of the current magnetic resonance elastography methods being used to characterize the elastic properties of soft tissues.**

64 Wong VW, Vergniol J, Wong GL *et al.* Diagnosis of fibrosis and cirrhosis using liver stiffness measurement in nonalcoholic fatty liver disease. *Hepatology* 51(2), 454–462 (2010).

65 Yoneda M, Suzuki K, Kato S *et al.* Nonalcoholic fatty liver disease: US-based acoustic radiation force impulse elastography. *Radiology* 256(2), 640–647 (2010).

66 Tanter M, Bercoff J, Athanasiou A *et al.* Quantitative assessment of breast lesion viscoelasticity: initial clinical results using supersonic shear imaging. *Ultrasound Med. Biol.* 34(9), 1373–1386 (2008).

67 McAleavey S, Collins E, Kelly J, Elegbe E, Menon M. Validation of SMURF estimation of shear modulus in hydrogels. *Ultrasonic Imaging* 31(2), 131–150 (2009).

68 McLaughlin J, Renzi D, Parker K, Wu Z. Shear wave speed recovery using moving interference patterns obtained in sonoelastography experiments. *J. Acoust. Soc. Am.* 121(4), 2438–2446 (2007).

69 McLaughlin J, Renzi D. Shear wave speed recovery in transient elastography and supersonic imaging using propagating fronts. *Inverse Problems* 22, 681–706 (2006).

70 McLaughlin J, Renzi D. Using level set based inversion of arrival times to recover shear wave speed in transient elastography and supersonic imaging. *Inverse Problems* 22, 707–725 (2006).

71 Muller M, Gennisson JL, Deffieux T, Tanter M, Fink M. Quantitative viscoelasticity mapping of human liver using supersonic shear imaging: preliminary *in vivo* feasibility study. *Ultrasound Med. Biol.* 35(2), 219–229 (2009).

72 Palmeri ML, Rouze NC, Wang MH, Ding X, Nightingale KR. Quantifying the impact of shear wavelength and kernel size on shear wave speed estimation. *Proceedings of the IEEE Ultrasonic Symposium.* San Diego, CA, USA, 11–14 October 2010.

73 Fahey BJ, Nelson RC, Hsu SJ, Bradway DP, Dumont DM, Trahey GE. *In vivo* guidance and assessment of liver radio-frequency ablation with acoustic radiation force elastography. *Ultrasound Med. Biol.* 34(10), 1590–1603 (2008).

74 Fahey BJ, Hsu SJ, Wolf PD, Nelson RC, Trahey GE. Liver ablation guidance with acoustic radiation force impulse imaging: challenges and opportunities. *Phys. Med. Biol.* 51, 3785–3808 (2006).

75 Fahey BJ, Nightingale KR, Stutz DL, Trahey GE. Acoustic radiation force impulse imaging of thermally-and chemically-induced lesions in soft tissues: preliminary *ex vivo* results. *Ultrasound Med. Biol.* 30(3), 321–328 (2004).

76 Bharat S, Techavipoo U, Kiss MZ, Liu M, Varghese T. Monitoring stiffness changes in lesions after radiofrequency ablation at different temperatures and durations of ablation. *Ultrasound Med. Biol.* 31(3), 415–422 (2005).

77 Jiang J, Varghese T, Brace CL *et al.* Young's modulus reconstruction for radio-frequency ablation electrode-induced displacement fields: a feasibility study. *IEEE Trans. Med. Imaging* 28(8), 1325–1334 (2009).

78 Zhang M, Castaneda B, Christensen J *et al.* Real-time sonoelastography of hepatic thermal lesions in a swine model. *Med. Phys.* 35(9), 4132–4141 (2008).

79 Krouskop T, Wheeler TM, Kallel F, Garra BS, Hall T. Elastic moduli of breast and prostate tissues under compression. *Ultrasonic Imaging* 20, 260–274 (1998).

80 Skovoroda A, Klishko AN, Gusakian DA *et al.* Quantitative analysis of the mechanical characteristics of pathologically changed soft biological tissues. *Biophysics* 40(6), 1359–1364 (1995).

81 Sandrin L, Fourquet B, Hasquenoph JM *et al.*. Transient elastography: a new noninvasive method for assessment of hepatic fibrosis. *Ultrasound Med. Biol.* 29(12), 1705–1713 (2003).

82 Di Ieva A, Grizzi F, Rognone E *et al.* Magnetic resonance elastography: a general overview of its current and future applications in brain imaging. *Neurosurg. Rev.* 33(2), 137–145 (2010).

83 Siegmann KC, Xydeas T, Sinkus R, Kraemer B, Vogel U, Claussen CD. Diagnostic value of MR elastography in addition to contrast-enhanced MR imaging of the breast-initial clinical results. *Eur. Radiol.* 20(2), 318–325 (2010).

84 Chopra R, Arani A, Huang YX *et al. In vivo* MR elastography of the prostate gland using a transurethral actuator. *Magn. Reson. Med.* 62(3), 665–671 (2009).

85 Tanter M, Bercoff J, Athanasiou A *et al.* Quantitative assessment of breast lesion viscoelasticity: initial clinical results using supersonic shear imaging. *Ultrasound Med. Biol.* 34(9), 1373–1386 (2008).

86 Righetti R, Righetti M, Ophir J, Krouskop TA. The feasibility of estimating and imaging the mechanical behavior of poroelastic materials using axial strain elastography. *Phys. Med. Biol.* 52(11), 3241–3259 (2007).

87 Righetti R, Garra BS, Mobbs LM, Kraemer-Chant CM, Ophir J, Krouskop TA. The feasibility of using poroelastographic techniques for distinguishing between normal and lymphedematous tissues *in vivo*. *Phys. Med. Biol.* 52(21), 6525–6541 (2007).

88 Leiderman R, Barbone PE, Oberai AA, Bamber JC. Coupling between elastic strain and interstitial fluid flow: ramifications for poroelastic imaging. *Phys. Med. Biol.* 51(24), 6291–6313 (2006).

89 Berry GP, Bamber JC, Mortimer PS, Bush NL, Miller NR, Barbone PE. The spatio-temporal strain response of oedematous and nonoedematous tissue to sustained compression *in vivo*. *Ultrasound Med. Biol.* 34(4), 617–629 (2008).

90 Zipparo M, Bing K, Nightingale K, Ultrasound imaging arrays with improved transmit power capability. *IEEE Trans. Ultrason. Ferroelectr. Freq. Control.* 57(9), 2076–2090 (2010).

91 Zheng Y, Chen S, Tan W, Kinnick R, Greenleaf JF. Detection of tissue harmonic motion induced by ultrasonic radiation force using pulse-echo ultrasound and Kalman filter. *IEEE Trans. Ultrason. Ferroelectr. Freq. Control.* 54(2), 290–300 (2007).

92 Urban MW, Chen S, Greenleaf JF. Error in estimates of tissue material properties from shear wave dispersion ultrasound vibrometry. *IEEE Trans. Ultrason. Ferroelectr. Freq. Control.* 56(4), 748–758 (2009).

93 Jiang J, Hall TJ. A generalized speckle tracking algorithm for ultrasonic strain imaging using dynamic programming. *Ultrasound Med. Biol.* 35(11), 1863–1879 (2009).

94 Bigelow TA, Church CC, Sandstrum K *et al.* The thermal index: its strengths, weaknesses, and proposed improvements. *J. Ultrasound Med.* 30, 714–734 (2011).

95 American Institue of Ultrasound in Medicine. Consensus report on potential bioeffects of diagnostic ultrasound. *J. Ultrasound Med.*27, 503–515 (2008).

96 Church CC, Carstensen EL, Nyborg WL, Carson PL, Frizzel LA, Bailey MR. The risk of exposure to diagnostic ultrasound in postnatal subjects: nonthermal mechanisms. *J. Ultrasound Med.* 27, 565–592 (2008).

97 O'Brien WD, Deng CX, Harris GR *et al.* The risk of exposure to diagnostic ultrasound in postnatal subjects: thermal effects. *J. Ultrasound Med.* 27(4), 517–535 (2008).

■ Websites

101 LOGIQ E9 Elastography www.gehealthcare.com/usen/ultrasound/genimg/products/logiq_e9/elastography.html (Accessed 8 December 2010)

102 Philips iU22 Elastography. 8 December 2010 www.healthcare.philips.com/in_en/products/ultrasound/technologies/elastography (Accessed 8 December 2010)